remote sensing

MDPI

Article

Feasibility of Acoustic Remote Sensing of Large Herring Shoals and Seafloor by Baleen Whales

Dong Hoon Yi and Nicholas C. Makris *

Department of Mechanical Engineering, Massachusetts Institute of Technology, Cambridge, MA 02139, USA; dongku@mit.edu

* Correspondence: makris@mit.edu; Tel.: +1-617-258-6104; Fax: +1-617-253-2350

Academic Editors: Deepak R. Mishra, Xiaofeng Li and Prasad S. Thenkabail
Received: 30 June 2016; Accepted: 16 August 2016; Published: 23 August 2016

Abstract: Recent research has found a high spatial and temporal correlation between certain baleen whale vocalizations and peak herring spawning processes in the Gulf of Maine. These vocalizations are apparently related to feeding activities with suggested functions that include communication, prey manipulation, and echolocation. Here, the feasibility of the echolocation function is investigated. Physical limitations on the ability to detect large herring shoals and the seafloor by acoustic remote sensing are determined with ocean acoustic propagation, scattering, and statistical theories given baleen whale auditory parameters. Detection is found to be highly dependent on ambient noise conditions, herring shoal distributions, baleen whale time-frequency vocalization spectra, and geophysical parameters of the ocean waveguide. Detections of large herring shoals are found to be physically feasible in common Gulf of Maine herring spawning scenarios at up to 10 ± 6 km in range for humpback parameters and 1 ± 1 km for minke parameters but not for blue and fin parameters even at zero horizontal range. Detections of the seafloor are found to be feasible up to 2 ± 1 km for blue and humpback parameters and roughly 1 km for fin and minke parameters, suggesting that the whales share a common acoustic sensation of rudimentary features of the geophysical environment.

Keywords: acoustic remote sensing; baleen whale; Atlantic herring; seafloor scattering

1. Introduction

Recent research has found a high spatial and temporal correlation between certain baleen whale vocalizations and peak annual spawning processes of Atlantic herring (*Clupea harengus*) in the Gulf of Maine [1,2], indicating an apparent relationship between these vocalizations and feeding activities of baleen whales. Suggested functions of the vocalizations include communication [3–6], prey manipulation [7], and echolocation [8–11], given the fact that Atlantic herring is a keystone prey species common in the diets of many marine animals including large whales in the Gulf of Maine region [12–14]. Here, feasibility of the possible echolocation function is investigated for large and dense herring aggregations. This differs substantially from the possible ability of baleen whales to detect other whales by active acoustics, which has been previously discussed [15–20].

The approach is to first determine parameters relevant to possible active acoustic sensing in baleen whales, including source and receiver characteristics such as time-frequency vocalization spectra and auditory system aperture. Detection of large herring shoals and the seafloor is then investigated using theoretical and numerical methods developed for analyzing Ocean Acoustic Waveguide Remote Sensing (OAWRS) of fish shoals [21–25] given these active sensing parameters. Sensing resolution in cross-range is determined by spatial array theory and in range by incoherent energy analysis [1,2,21–26], since evidence suggests temporally coherent auditory processing is unlikely [27,28].

Typical well documented scenarios during the herring spawning season on Georges Bank [1,2,22,24,25] are investigated to determine ranges up to which detection of large herring shoals

and the seafloor is feasible for given whale acoustic parameters. Detection of large herring shoals and the seafloor is found to be highly dependent on local ambient noise conditions at whale locations, herring shoal distribution, baleen whale vocalization parameters such as time duration and source spectra, as well as oceanographic conditions including sound speed structure, bathymetry, and seafloor scattering amplitudes along the acoustic propagation path.

2. Materials and Methods

2.1. Acoustic Parameters Relevant to Potential Active Acoustic Sensing in Baleen Whales and Corresponding Spatial Resolution

Baleen whale vocalization for potential active sensing is parameterized by call source level SL, time duration T, center frequency $\bar{f}$, and one-third octave frequency bandwidth $BW_{1/3}$ with center frequency $\bar{f}$ (Table 1) following conventions for measuring these parameters in References [1–4].

For potential active sensing, a baleen whale's acoustic receiver is parameterized as a two-element spatially coherent array of omni-directional receivers of aperture L corresponding to the separation between ears, which is consistent with the small ear-dimensions to wavelength ratio of vocalizations and the low impedance contrast between tissue and sea water. The corresponding far-field beam pattern is obtained by spatial array theory (Figure 1) as:

$$B(\sin\theta) = \cos\left(\frac{\pi f L}{c}\sin\theta\right) \tag{1}$$

where θ is the angle from array broadside, f is the frequency, and c is the sound speed. The aperture and frequency are taken from Table 1 for the baleen whales considered. The angular resolution of this two element array is best for broadside steering and is given by equivalent beamwidth:

$$d\theta = 2\sin^{-1}(\psi/2) \tag{2}$$

where

$$\psi = \int_{-1}^{1} |B(\sin\theta)|^2 d(\sin\theta) = 1 + \frac{c}{2\pi f L}\sin\left(\frac{2\pi f L}{c}\right) \tag{3}$$

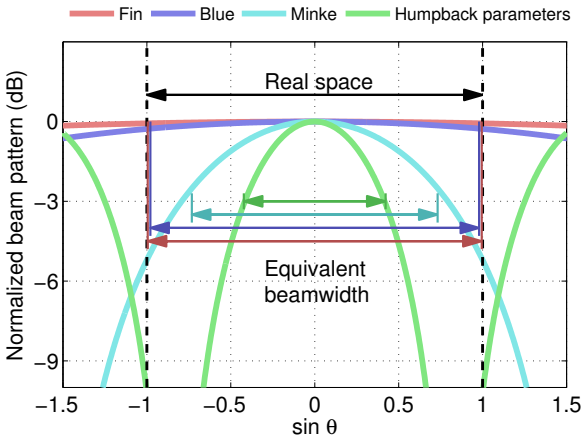

Figure 1. Beam patterns of two-element coherent array steered at broadside given baleen whale acoustic parameters given in Table 1.

Cross-range resolution is then determined as $\rho d\theta$ at array broadside, at horizontal range ρ, for an effectively monostatic active sensing system. No ambiguity in directional sensing due to grating lobes [29] is expected because the grating lobes are located outside real space for given whale acoustic

parameters (Table 1). Assuming incoherent energy analysis, range resolution $d\rho$ is $\frac{cT}{2}$, where the active signal duration T is given in Table 1 for the various baleen whales considered. The areal resolution of the parameterized active sensing system or the smallest area distinguishable by the sensing system, typically referred to as the resolution footprint, is then given by $\rho d\rho d\theta$ for monostatic geometries (Figure 2).

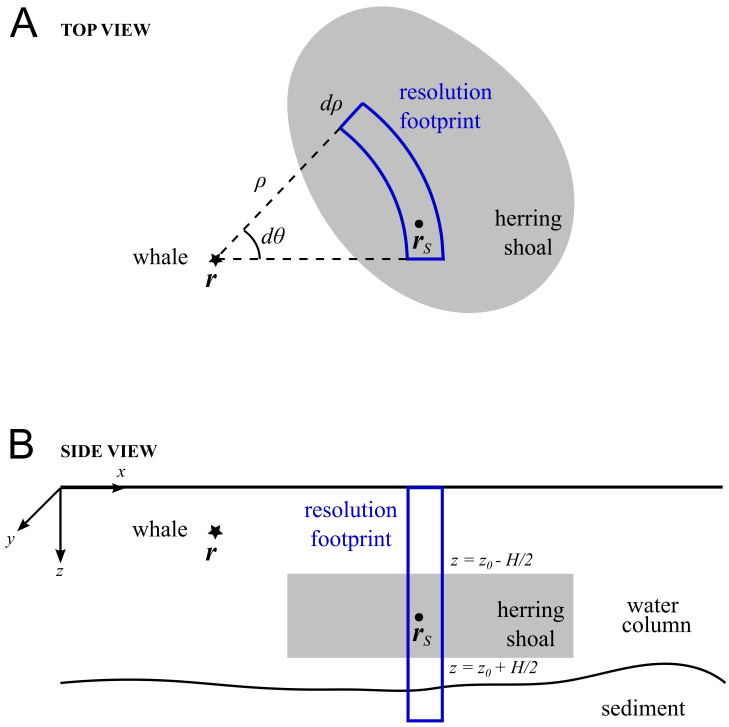

Figure 2. Top view (**A**) and side view (**B**) of the geometry for possible acoustic remote sensing in a continental shelf environment by baleen whales. The resolution footprint given baleen whale acoustic parameters is an annular sector with range extent $d\rho$ and cross-range extent $\rho d\theta$.

2.2. Detection of Scattered Returns from Herring Shoals and the Seafloor

The expected magnitude square of the scattered field, $\langle |\Phi_F|^2 \rangle$, received at location $\mathbf{r}$ from N omni-directional targets randomly distributed with uniform probability in a vertical layer of thickness H centered at $z = z_0$ within a resolution footprint $A_R(\boldsymbol{\rho_C})$ centered at horizontal location $\boldsymbol{\rho_C}$ can be determined from [23,30]:

$$10 \log_{10} \left\langle \left| \frac{\Phi_F}{\Phi_{ref}} \right|^2 \right\rangle \approx SL + TLA + TS + 10 \log_{10} \frac{\langle n_A \rangle}{n_{A,ref}} \tag{4}$$

In Equation (4), $\Phi_{ref} = 1$ μPa is the reference acoustic pressure in water, SL is the whale call source level with mean and standard deviation [1,2] given in Table 1 consistent with circular complex Gaussian random fields fluctuations [26], TLA is the depth-averaged two-way transmission loss to individual targets integrated over one resolution footprint area [23] given in Equation (5), $TS = 10 \log_{10} \left\langle \left| \frac{S}{r_{ref} k} \right|^2 \right\rangle$ is the expected target strength of a single herring, S is the plane wave scatter function of a single herring, k is the acoustic wavenumber, $r_{ref} = 1$ m is the reference length, $n_{A,ref} = 1$ fish/m^2 is the reference areal fish population density, and $\langle n_A \rangle = N / A_R(\boldsymbol{\rho_C})$ is the expected areal density of the targets within a spatially varying resolution cell centered at horizontal location $\boldsymbol{\rho_C}$. When the instantaneous bandwidth BW of baleen whale vocalizations [1,2] is greater than the one-third octave bandwidth $BW_{1/3}$ given in

Table 1, an adjusted whale call source level $SL_{adj} = SL + 10\log_{10}\frac{BW_{1/3}}{BW}$ is used. The expected target strength of a single herring in a vertical layer is determined by parameters such as mean layer depth, shoal thickness, neutral buoyancy depth, and herring length. With mean and standard deviation of the parameters empirically determined in Reference [24] (Table 2), TS is determined using a swimbladder resonance model [31] for deep shoals as described in Appendix A. Similar analysis is performed for shallow shoals given measured constraints. The TLA term in Equation (4) can be written [23] for monostatic sensing as:

$$TLA = 10\log_{10}\left(\int_{A_R(\boldsymbol{\rho}_C)}\frac{1}{H}\int_{z_0-H/2}^{z_0+H/2}(4\pi)^4\langle|G(\mathbf{r}|\boldsymbol{\rho}_S,z_S;f,c(\mathbf{r_w}),d(\mathbf{r_w}))|^4|\boldsymbol{\rho}_S,z_S\rangle \mathrm{d}\mathbf{z_S}\mathrm{d}{\boldsymbol{\rho}_S}^2/r_{ref}^{-2}\right) \quad (5)$$

where $G(\mathbf{r}|\boldsymbol{\rho}_S,z_S;f,c(\mathbf{r_w}),d(\mathbf{r_w}))$ is the Green function between the target location $\mathbf{r_S} = (\boldsymbol{\rho}_S,z_S)$ and the receiver location $\mathbf{r}$, and $c(\mathbf{r_w})$ and $d(\mathbf{r_w})$ are the sound speed and the density in the water column at any point $\mathbf{r_w}$ in the propagation path, respectively. The areal integration in Equation (5) should be taken over the intersection between resolution footprint and the area occupied by herring when the herring distribution does not fully overlap with the resolution footprint. A parabolic equation model [32] is used to calculate the Green function from the whale location to the herring shoal in a range-dependent Gulf of Maine environment. The conditional expectation over the sound speed and the density in Equation (5) is determined by averaging 10 Monte-Carlo realizations, where the Green functions are calculated along the entire propagation path in range and depth for each realization. Each Monte-Carlo realization employs a different sound speed profile measured during the OAWRS 2006 experiment [24] every 500 m [33,34] along the propagation path.

Table 1. Parameters of baleen whale's auditory reception and signal detection used for detection range estimation in the Gulf of Maine scenario.

Baleen Whale Species	SL (dB re 1 μPa 1 m)	T (s)	$\bar{f}$ (Hz)	$BW_{1/3}$ (Hz)	DT (dB)	AG (dB)	L (m)	α $\left(\frac{\mathrm{Pa}^2}{(1\ \mu\mathrm{Pa})^2(\mathrm{m/s})^n}\right)$	β $\left(\frac{\mathrm{Pa}^2}{(1\ \mu\mathrm{Pa})^2}\right)$	n
Fin	189 ± 5.6	0.8	20	5	3	0	3	1.88×10^8	6.68×10^5	0.6
Blue	189 ± 5.6	2	40	10	3	0	3	1.19×10^8	2.51×10^6	0.4
Minke	179 ± 5.6	0.1	315	72.5	3	1.4	1.5	5.96×10^6	3.76×10^5	0.6
Humpback	180 ± 5.6	1.44	450	100	3	3.7	2	1.26×10^6	5.01×10^6	1.1

SL is the whale call source level [1], T is the time duration, $\bar{f}$ is the center frequency of baleen whale vocalizations relevant for target detection, $BW_{1/3}$ is the one-third octave bandwidth centered at frequency $\bar{f}$, DT is the detection threshold, AG is the array gain given whale acoustic parameters, L is the spatial distance between the two omni-directional receiver with spatial coherence, α is the waveguide propagation factor [35], β is the constant baseline ambient noise intensity, and n is the power law coefficient of wind-speed-dependent ambient noise. The parameter values for SL are given in the form of mean $\pm$ standard deviation.

Table 2. Parameters of herring shoals.

Herring Shoals	z_0 (m)	H (m)	z_{nb} (m)	l (cm)	$\langle n_A \rangle$ (fish/m^2)
Deep	155 ± 6.5	50 ± 15.6	83 ± 31.3	24.2 ± 1.7	5.0
Shallow	25 ± 1.0	20 ± 6.2	20 ± 6.5	24.2 ± 1.7	1.0

z_0 is the mean depth of herring layer, H is the shoal thickness, z_{nb} is the neutral buoyancy depth of herring, l is the fork length of herring, and n_A is the areal population density of herring shoals. The parameter values for z_0, H, z_{nb}, and l are given in the form of mean $\pm$ standard deviation.

The expected magnitude square of the scattered field $\langle|\Phi_S|^2\rangle$ from the seafloor is determined from [25]:

$$10\log_{10}\left\langle\left|\frac{\Phi_S}{\Phi_{ref}}\right|^2\right\rangle \approx SL + 10\log_{10}\left(\iiint_{V_R(\boldsymbol{\rho_C})}(4\pi)^2\langle|G(\mathbf{r}|\mathbf{r_S};f,c(\mathbf{r_w}),d(\mathbf{r_w}))|^4|\mathbf{r_S}\rangle d\mathbf{r_S}^3/r_{ref}^{-1}\right) + 10\log_{10}\left(\left\langle|A_S(f,\Gamma_\kappa,\Gamma_d,V_C)|^2\right\rangle/r_{ref}^{-1}\right) \quad (6)$$

where SL is the whale call source level, $V_R(\boldsymbol{\rho_C})$ is the volume of the resolution cell centered at horizontal location $\boldsymbol{\rho_C}$, $G(\mathbf{r}|\boldsymbol{r_S};f,c(\mathbf{r_w}),d(\mathbf{r_w}))$ is the Green function between the target location $\mathbf{r_S} = (\boldsymbol{\rho_S}, z_S)$ and the receiver location $\mathbf{r}$, $c(\mathbf{r_w})$ and $d(\mathbf{r_w})$ are the sound speed and the density at any point $\mathbf{r_w}$ in the propagation path, respectively. The Green function and the conditional expectation over the water column sound speed and the density in Equation (6) are determined by following the same procedures given for those in Equation (5). The expected magnitude square of Rayleigh-Born seafloor scattering amplitude per coherence volume $\langle|A_S(f,\Gamma_\kappa,\Gamma_d,V_C)|^2\rangle$ is defined as [25]:

$$\langle|A_S(f,\Gamma_\kappa,\Gamma_d,V_C)|^2\rangle = k^4V_C\left[\mathrm{Var}(\Gamma_\kappa) + F_d\mathrm{Var}(\Gamma_d) + F_c\mathrm{Cov}(\Gamma_\kappa,\Gamma_d)\right] \quad (7)$$

where Γ_κ is the fractional change in seafloor compressibility, Γ_d is the fractional change in seafloor density, V_C is the coherence volume of inhomogeneities, and F_κ and F_d are the proportionality constants of scattering contributions from dipole and cross terms to monopole scattering contributions, respectively. The frequency dependence of the expected magnitude square of Rayleigh-Born seafloor scattering amplitude per coherence volume $\langle|A_S(f,\Gamma_\kappa,\Gamma_d,V_C)|^2\rangle$ is measured during the OAWRS 2006 experiment [25] as:

$$\langle|A_S(f,\Gamma_\kappa,\Gamma_d,V_C)|^2\rangle = C\times f^q \quad (8)$$

where $C \approx 1.78\times10^{-8}$ m^{-1} Hz^{-q} is the proportionality constant, f is the frequency, and $q \approx 2.12$ is the power law coefficient of frequency dependence of the expected magnitude square of the seafloor scattering amplitude. The level of magnitude square of Rayleigh-Born seafloor scattering amplitude per coherence volume is assumed to vary with standard deviation up to 2 dB as empirically determined in Reference [25].

The expected magnitude square of ambient noise field is determined as [1,2]:

$$\langle|\Phi_N|^2\rangle \approx \frac{1}{\tau}\int_{BW_{1/3}}|\Phi_N^{data}(f)|^2df \approx \frac{1}{\tau}|\Phi_N^{data}(\bar{f})|^2\times BW_{1/3} \quad (9)$$

where τ is the measurement time, f is the frequency, $\Phi_N^{data}(f)$ is the Fourier transform of the measured ambient noise field time series, $\Phi_N^{data}(\bar{f})$ is the Fourier transform of the measured ambient noise field time series evaluated at the center frequency $\bar{f}$ of baleen whale vocalizations given in Table 1, and $BW_{1/3}$ is the one-third octave frequency bandwidth of various baleen whale vocalizations given in Table 1. The expected magnitude square of the beamformed ambient noise field $\Phi_{N,BF}$ is determined from:

$$10\log_{10}\frac{\langle|\Phi_N|^2\rangle}{\langle|\Phi_{N,BF}|^2\rangle} = AG \quad (10)$$

where AG is the array gain of the receiver array given in Table 1. The wind-speed dependence of ambient noise is modeled as [2]:

$$\left\langle\left|\frac{\Phi_N}{\Phi_{ref}}\right|^2\right\rangle = \alpha v^n + \beta \quad (11)$$

where $\Phi_{ref} = 1$ μPa is the reference acoustic pressure in water, v is the wind speed, n is the power law coefficient of wind-speed-dependent ambient noise, α is the waveguide propagation factor [35], and β is the constant baseline ambient noise intensity. The coefficients n, α, and β given in Table 1 are

empirically determined [2] by least-square fitting between the measured and the modeled ambient noise levels as a function of measured wind speed during the OAWRS 2006 experiment [22] (Figure A1). The instantaneous measurements of ambient noise vary with 5.6 dB standard deviation [26].

For target detection under seafloor scattering limited detection conditions, the expected magnitude square of the scattered field from herring shoals should be greater than that of the scattered field from the seafloor by a factor that corresponds to detection threshold DT given in Table 1:

$$10 \log_{10} \frac{\langle |\Phi_F|^2 \rangle}{\langle |\Phi_S|^2 \rangle} \geq DT \tag{12}$$

where the maximum detection range is found when the equality holds. Similarly for target detection under noise limited conditions, the expected magnitude square of the scattered field from herring shoals should be greater than that of the beamformed ambient noise field $\Phi_{N,BF}$ by a factor that corresponds to DT given in Table 1:

$$10 \log_{10} \frac{\langle |\Phi_F|^2 \rangle}{\langle |\Phi_{N,BF}|^2 \rangle} \geq DT \tag{13}$$

where the maximum detection range is found when the equality holds. The detection threshold DT is determined by requiring that the scattered returns from fish targets stand at least one standard deviation [26,36] above background levels from seafloor scattering or ambient noise.

2.3. OAWRS Experiment during Peak Herring Spawning Processes in the Gulf of Maine in Fall 2006

An OAWRS experiment was conducted on the northern flank of Georges Bank during the peak annual Atlantic herring spawning period in the Fall of 2006 [1,22,24]. The spatial distribution of herring was instantaneously imaged and continuously monitored [22]. The spawning process was found to follow a regular diurnal pattern, where herring were diffusely scattered near the seafloor during daylight hours, formed dense and large shoals near the 180–200 m depth contours near sunset, and then migrated synchronously towards spawning grounds at depths less than 50 m in the evening as shown in Figure 3A [22].

Parabolic equation transmission loss modeling [32] was calibrated and verified with roughly one hundred two-way transmission loss measurements made from calibrated targets with known scattering properties [37] and thousands of one-way transmission loss measurements [24,36] during the same experiment. Herring target strength was determined by empirical fit to a resonance model [31] over multi-frequencies in ranges relevant to this study [24]. Thousands of baleen whale vocalizations were passively recorded and localized in the vicinity of large herring shoals and call parameters, as shown in Table 1, were determined [1,2]. Ambient noise levels that include wind-driven and shipping noise contributions were measured and fit to empirical models at baleen whale vocalization frequencies [1,2].

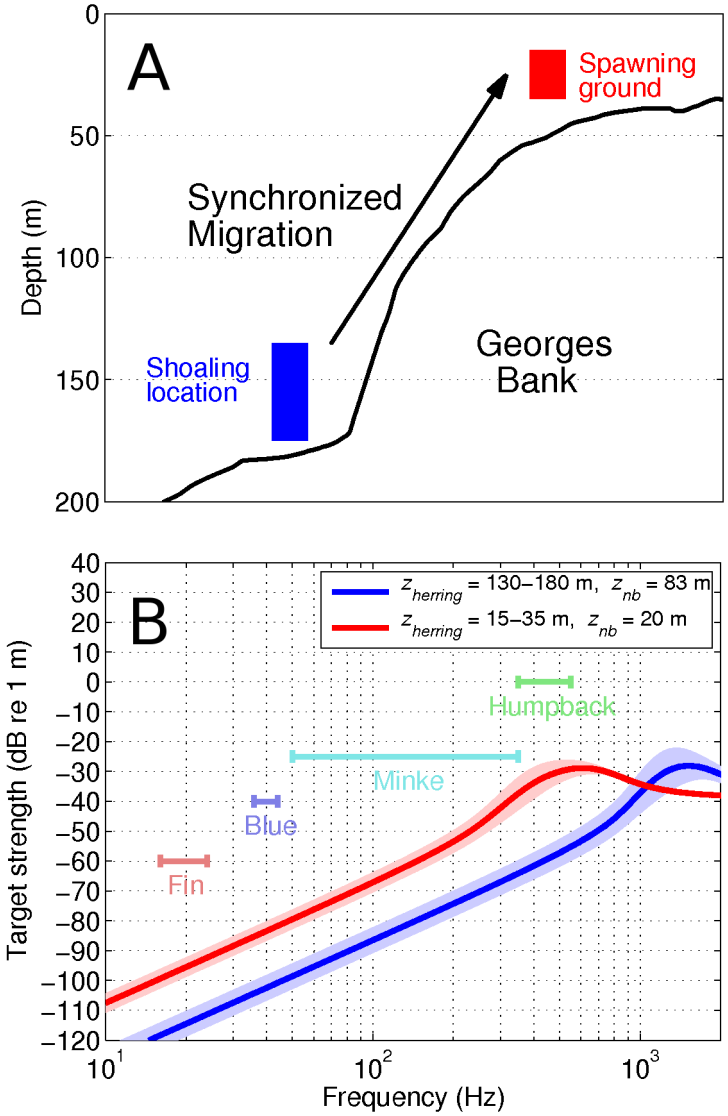

Figure 3. (**A**) Migration of herring shoals from depths greater than 100 m to less than 50 m in the Gulf of Maine; (**B**) Corresponding frequency dependence of resonance scattering of herring swimbladders for deep and shallow shoals. Blue and red solid lines represent the herring target strength when herring layer is at depths $z_{herring}$ of 130–180 m with a neutral buoyancy depth z_{nb} of 83 m on the northern flank of Georges Bank and at depths $z_{herring}$ of 15–35 m with a neutral buoyancy depth z_{nb} of 20 m on Georges Bank, respectively.

3. Results

We find acoustic detections of herring shoals are physically feasible up to 10 ± 6 km in range for humpback (*Megaptera novaeangliae*) parameters and 1 ± 1 km for minke (*Balaenoptera acutorostrata*) parameters in common herring spawning scenarios of dense near-surface concentrations at 15–35 m depth, but not for herring concentrations at 130–180 m depth even at zero horizontal range (Figures 4 and 5). This assumes detections are possible when scattered returns from herring shoals stand at least one standard deviation above mean ambient noise and seafloor scattering levels, and the measured ambient noise conditions, herring shoal distributions, baleen whale time-frequency vocalization spectra, and geophysical parameters of the ocean waveguide in the Gulf of Maine during the 2006 herring spawning period. The detection range of 1 ± 1 km, where spherical spreading dominates, suggests that the corresponding minke parameters are better suited to

direct-path waterborne rather than waveguide acoustic sensing. For fin (*Balaenoptera physalus*) and blue (*Balaenoptera musculus*) parameters, we find detection of herring shoals is not feasible even at zero horizontal range (Figures 4 and 5) for any of the shoal depths considered because the scattered intensity from the shoals is at least two orders of magnitude lower than those from the seafloor.

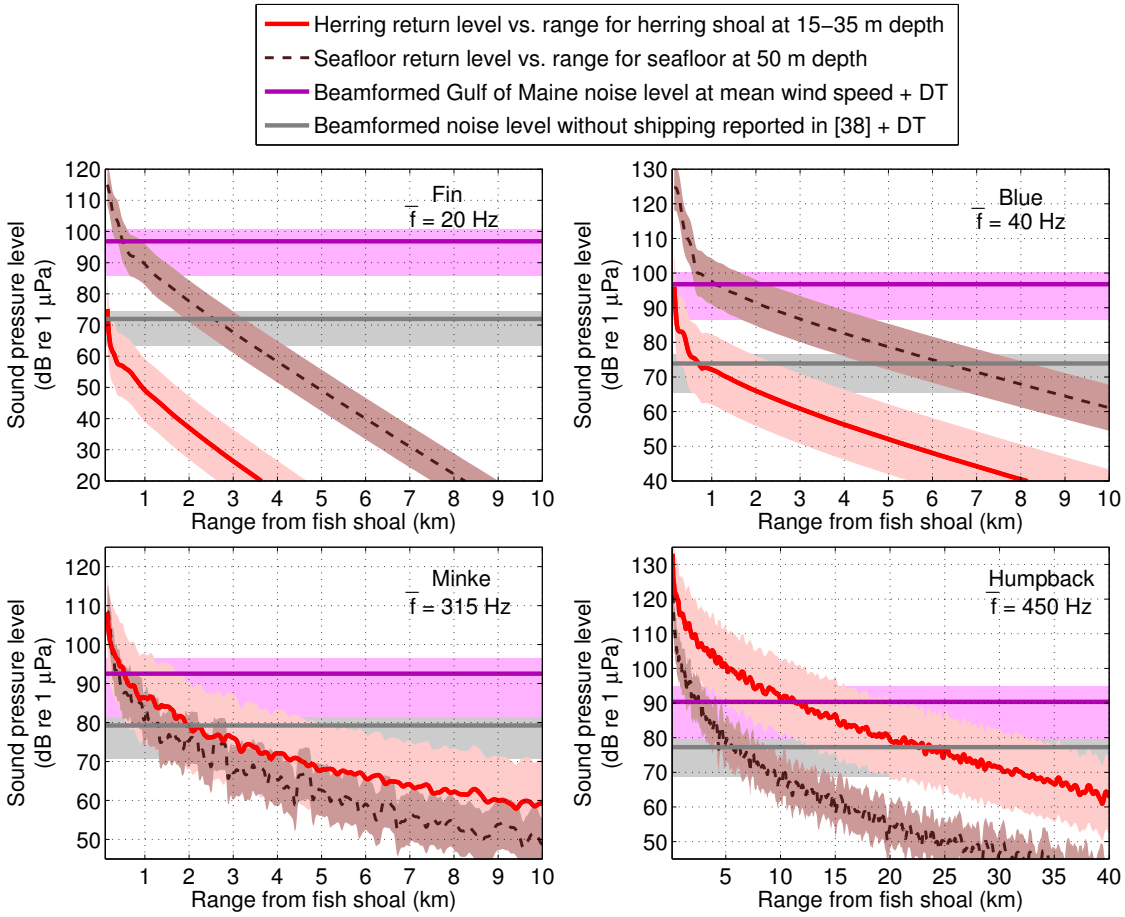

Figure 4. Detections of herring shoals are feasible up to 10 ± 6 km in range for humpback parameters and 1 ± 1 km for minke parameters in common Gulf of Maine herring spawning scenarios of dense near-surface concentrations at depths of 15–35 m (red solid lines). Detections of the seafloor are found to be feasible up to 2 ± 1 km in range for blue and humpback parameters and roughly 1 km for fin and minke parameters over local ambient noise. Dark red dashed lines represent seafloor scattering for a seafloor depth of 50 m. Purple solid lines represent the beamformed ambient noise levels with mean wind speed of 5.6 m/s during peak herring spawning period in the Gulf of Maine with one detection threshold (*DT*) added. Light purple shaded areas range from the beamformed ambient noise levels at 2 m/s wind speed minus 5.6 dB to those at 10 m/s wind speed plus 5.6 dB, to illustrate the typical range of wind-speed-dependent ambient noise encountered. Gray solid lines represent the beamformed ambient noise level without significant shipping with wind speed of 5.1 m/s [38] with one *DT* added. Light gray shaded areas range from beamformed ambient noise levels without significant shipping at 5.1 m/s wind speed plus/minus the instantaneous intensity standard deviation of 5.6 dB. The beamformed ambient noise levels are determined for frequency bands of baleen whale vocalizations given in Table 1 using Equations (9) and (10).

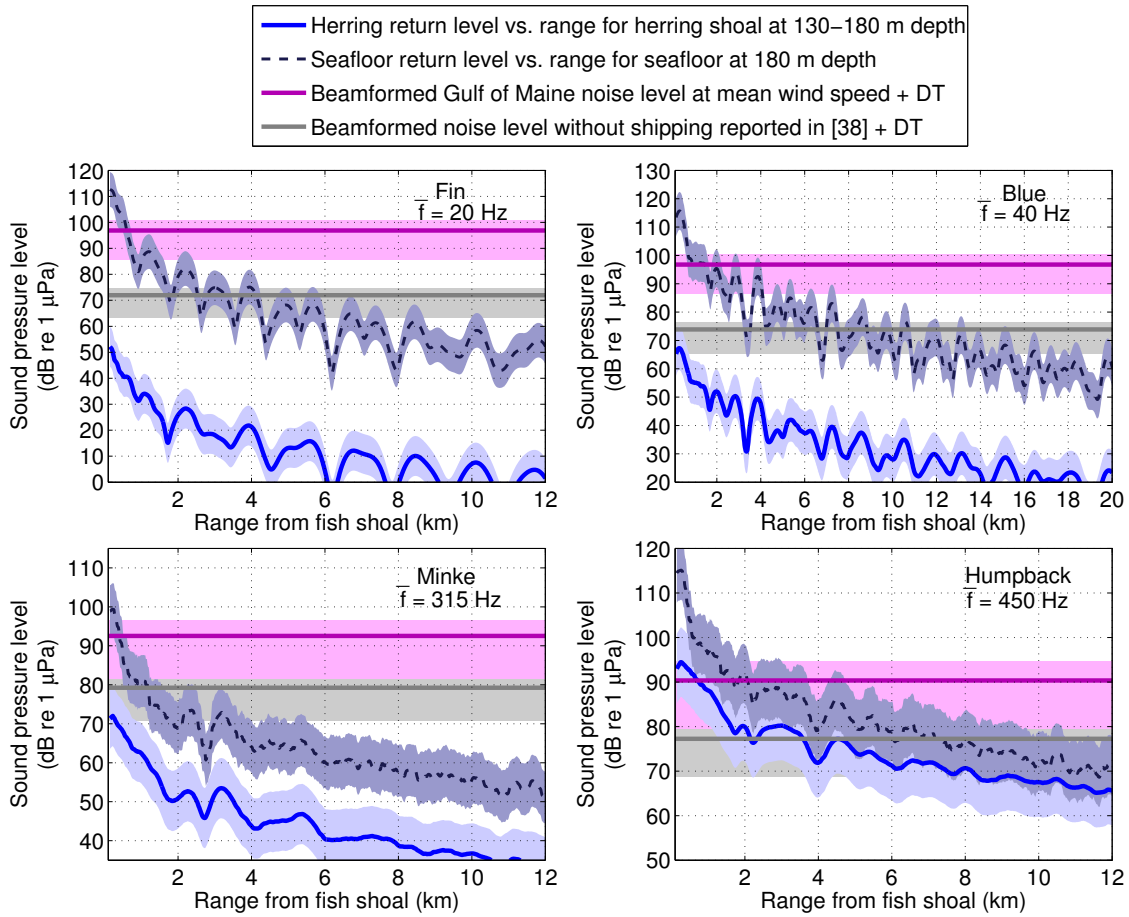

Figure 5. Detections of herring shoals at depths of 130–180 m (blue solid lines) are found to be unfeasible for the parameters of any baleen whale considered. Detections of the seafloor are found to be feasible up to 2 ± 1 km in range for blue and humpback parameters and roughly 1 km for fin and minke parameters over local ambient noise. Dark blue dashed lines represent seafloor scattering for a seafloor depth of 180 m. Purple solid lines represent the beamformed ambient noise levels with mean wind speed of 5.6 m/s during peak herring spawning period in the Gulf of Maine with one detection threshold (DT) added. Light purple shaded areas range from the beamformed ambient noise levels at 2 m/s wind speed minus 5.6 dB to those at 10 m/s wind speed plus 5.6 dB, to illustrate the typical range of wind-speed-dependent ambient noise encountered. Gray solid lines represent the beamformed ambient noise level without significant shipping with wind speed of 5.1 m/s [38] with one DT added. Light gray shaded areas range from beamformed ambient noise levels without significant shipping at 5.1 m/s wind speed plus/minus the instantaneous intensity standard deviation of 5.6 dB. The beamformed ambient noise levels are determined for frequency bands of baleen whale vocalizations given in Table 1 using Equations (9) and (10).

The observed variations in detection range are most strongly affected by the frequency dependence of resonant scattering from herring swimbladders. For shallow shoals, whale frequency ranges closer to the resonant scattering peak lead to greater detection ranges (Figure 3B). For deep shoals, all whale frequency ranges considered are too far below the resonant scattering peak to lead to detections. As herring shoals migrate to the south from the deep locations on the northern flank of Georges Bank to shallower than 50 m on Georges Bank (Figure 3A), it is found that the resonant frequency of herring swimbladders shifts to lower frequencies from roughly 1.5 kHz to roughly 600 Hz (Figure 3B). Herring target strength at baleen whale vocalization frequencies then increases by roughly two orders

of magnitude (Figure 3B), which is the key factor enabling active acoustic detection of herring shoals for minke and humpback parameters.

We find seafloor detection is physically feasible up to 2 ± 1 km in range for blue and humpback parameters and roughly 1 km for fin and minke parameters. This assumes scattered returns from the seafloor stand at least one standard deviation above ambient noise levels (Figures 4 and 5). This suggests that the baleen whales share a common acoustic sensation of rudimentary features of the geophysical environment.

4. Discussion

Little information exists on the mechanisms by which baleen whales detect prey [28,39,40]. Since the current analysis does not examine behavioral data, no conclusions can be drawn about whether the baleen whales considered actually employ active sensing to detect herring shoal prey. The analysis merely considers the physical feasibility of such sensing from an acoustic detection perspective. It is interesting, however, that the whale vocalization spectra do not appear to be optimized to take advantage of the peak resonant target strength of the deeper herring shoals, and only the humpback and perhaps the minke spectra are situated at or near the resonant peak for the shallower shoals.

Our analysis shows that local ambient noise is the primary limiting factor in detection of herring shoals for humpback and minke parameters as well as seafloor detections for the parameters of any whale considered (Figures 4 and 5). It is possible that detections of herring shoals would then be feasible at much longer ranges under ocean ambient noise conditions without significant shipping traffic [38,41]. For example, under ambient noise conditions reported for Arafura and Timor Seas in Australia [38] with insignificant shipping, detections of herring shoals would be feasible up to 10–30 km in range for humpback parameters and 2–5 km for minke parameters (Figure 4). Similarly, detections of the seafloor would be feasible up to 5–8 km in range for blue parameters, 4–9 km for humpback parameters, 2–4 km for fin parameters, and 1–3 km for minke parameters (Figures 4 and 5) under ocean ambient noise conditions without significant shipping. These estimates could represent possible detection ranges in ancient ocean environments that lacked shipping noise contributions.

5. Conclusions

The feasibility of acoustic remote sensing of large herring shoals and the seafloor by baleen whales has been investigated. We have found that it is physically feasible to detect dense near-surface herring shoals up to 10 ± 6 km in range with humpback acoustic parameters and 1 ± 1 km with minke acoustic parameters over ambient noise and seafloor scattering levels in the Gulf of Maine continental shelf environment. In contrast, detections of herring shoals are found to be unfeasible for fin and blue whale parameters even at zero horizontal range because scattered intensity from the seafloor are expected to be greater than the scattered intensity from herring shoals. These variations in detection range are primarily due to the strong frequency dependence of resonant scattering from herring swimbladders. We have found that detections of the seafloor are feasible up to 2 ± 1 km in range for blue and humpback parameters and roughly 1 km for fin and minke parameters over ambient noise, suggesting that the whales share a common acoustic sensation of rudimentary features of the geophysical environment.

Acknowledgments: The basic concept of the paper arose from independent suggestions by Peter Tyack and Purnima Ratilal, who we thank for many useful discussions. This research was supported by the Office of Naval Research.

Author Contributions: Dong Hoon Yi and Nicholas C. Makris developed the approach, analyzed the data, and wrote the paper.

Conflicts of Interest: The authors declare no conflict of interest.

Appendix A. Estimation of Expected Target Strength of a Single Herring in a Vertical Layer

The probability density function of a Gaussian variable x with mean μ and standard deviation σ_x is:

$$f(x|\mu,\sigma_x^2) = \frac{1}{\sqrt{2\pi\sigma_x^2}} e^{-\frac{(x-\mu)^2}{2\sigma_x^2}} \tag{A1}$$

with a cumulative distribution function:

$$F(x) = \frac{1}{2}\left[1 + \mathrm{erf}\left(\frac{x-\mu}{\sigma_x\sqrt{2}}\right)\right] \tag{A2}$$

where $\mathrm{erf}(x) = \frac{1}{\sqrt{\pi}}\int_{-x}^{x} e^{-t^2} dt$.

When the variable x is truncated within $x_{low} < x < x_{high}$ where x_{low} and x_{high} are determined to ensure positiveness of the parameters for target strength estimation of a single herring in a vertical layer, the probability density function $g(x)$ for the truncated Gaussian distribution is expressed as:

$$g(x|\mu,\sigma_x^2,x_{low},x_{high}) = \frac{1}{\sqrt{2\pi\sigma_x^2}} e^{-\frac{(x-\mu)^2}{2\sigma_x^2}} \frac{1}{F(x_{high}) - F(x_{low})} \tag{A3}$$

This distribution is assumed for mean depth of herring shoal z_0, shoal thickness H, neutral buoyancy depth z_{nb}, and herring length with mean μ and standard deviation σ_x given in Table 2.

Using a fish swimbladder resonance model [23,31], the expected target strength TS of a single herring in a uniform vertical layer of herring is determined from:

$$\begin{aligned}\left\langle \left|\frac{S}{k}\right|^2 \right\rangle &= \iiiint \frac{1}{H}\int_{z_0-H/2}^{z_0+H/2} \left|\frac{S}{k}\right|^2 dz g(z_0) dz_0 g(H) dH g(l) dl g(z_{nb}) dz_{nb} \\ &= \iiiint \frac{1}{H}\int_{z_0-H/2}^{z_0+H/2} \frac{r^2(z,z_{nb},l)}{\frac{f_0^2(z,z_{nb},l)}{f^2}\eta^{-2}(z,z_{nb},l,f) + \left(\frac{f_0^2(z,z_{nb},l)}{f^2} - 1\right)^2} dz g(l) dl g(z_0) dz_0 g(H) dH g(z_{nb}) dz_{nb}\end{aligned} \tag{A4}$$

where S is the plane wave scatter function of a single herring, k is the acoustic wavenumber, f is the frequency, z is the herring depth, l is the fork length of herring, $r(z,z_{nb},l)$ is the equivalent radius of swimbladder, $f_0(z,z_{nb},l)$ is the resonant frequency of swimbladder, $\eta(z,z_{nb},l,f)$ is the damping factor, $TS = 10\log_{10}\left\langle \left|\frac{S}{r_{ref}k}\right|^2 \right\rangle$, and $r_{ref} = 1$ m is the reference length. In Equation (A4), the equivalent radius of swimbladder $r(z,z_{nb},l)$ is determined by:

$$r(z,z_{nb},l) = \left[\frac{3}{4\pi}\frac{c_{nb}m_{flesh}(l)}{\rho_{flesh}}\frac{1+z_{nb}/10}{1+z/10}\right]^{1/3} \tag{A5}$$

assuming that the swimbladder volume varies with pressure according to Boyle's law [42], where c_{nb} is the ratio of the swimbladder volume at neutral buoyancy to the volume of herring's flesh V_{flesh} assumed to be 0.05 [43], $V_{flesh} = m_{flesh}(l)/\rho_{flesh}$, $m_{flesh}(l)$ is the mass of a single herring empirically determined by the fork length of herring l as $3.35\times10^{-6}l^{3.35}$ in kg when l is given in cm [24], and ρ_{flesh} is the density of herring's flesh of 1071 kg/m^3 [44]. The resonant frequency of herring swimbladder $f_0(z,z_{nb},l)$ in Equation (A4) is determined by:

$$f_0(z,z_{nb},l) = \frac{\kappa(\epsilon(z,z_{nb},l))}{2\pi r(z,z_{nb})}\sqrt{\frac{3\gamma P_{atm}(1+z/10)}{\rho_{flesh}}} \tag{A6}$$

where $\gamma = 1.4$ is the ratio of the specific heats of air, and $P_{atm} = 1.013\times10^5$ Pa is the atmospheric pressure, $\kappa(\epsilon(z,z_{nb},l))$ is the swimbladder correction term, and $\epsilon(z,z_{nb},l)$ is the

swimbladder's eccentricity. The correction term $\kappa(\epsilon(z, z_{nb}, l))$ for a prolate spheroidal swimbladder [45] is given by:

$$\kappa(\epsilon(z, z_{nb}, l)) = \frac{\sqrt{2}(1 - \epsilon^2(z, z_{nb}, l))^{1/4}}{\epsilon^{1/3}(z, z_{nb}, l)} \left[\ln \left(\frac{1 + \sqrt{1 + \epsilon^2(z, z_{nb}, l)}}{1 - \sqrt{1 - \epsilon^2(z, z_{nb}, l)}} \right) \right]^{-1/2} \quad \text{(A7)}$$

In Equation (A7), the ratio of the minor to major axis of a prolate spheroidal swimbladder $\epsilon(z, z_{nb}, l)$ is $\left(\frac{c_{sb} l/2}{r(z, z_{nb}, l)} \right)^{3/2}$, and the ratio between the herring's fork length l and the major axis of the swimbladder is assumed to be $c_{sb} \approx 0.364$ for herring [24]. The damping factor $\eta(r, r_{nb}, l, f)$ in Equation (A4) is obtained from:

$$\frac{1}{\eta(z, z_{nb}, l, f)} = \frac{2\pi r(z, z_{nb}, l) f^2}{c f_0(z, z_{nb}, l)} + \frac{\xi}{\pi r^2(z, z_{nb}, l) f_0(z, z_{nb}, l) \rho_{flesh}} \quad \text{(A8)}$$

where f is the frequency, c is the sound speed, and ξ is the viscosity of herring's flesh given to be 50 Pa s [44].

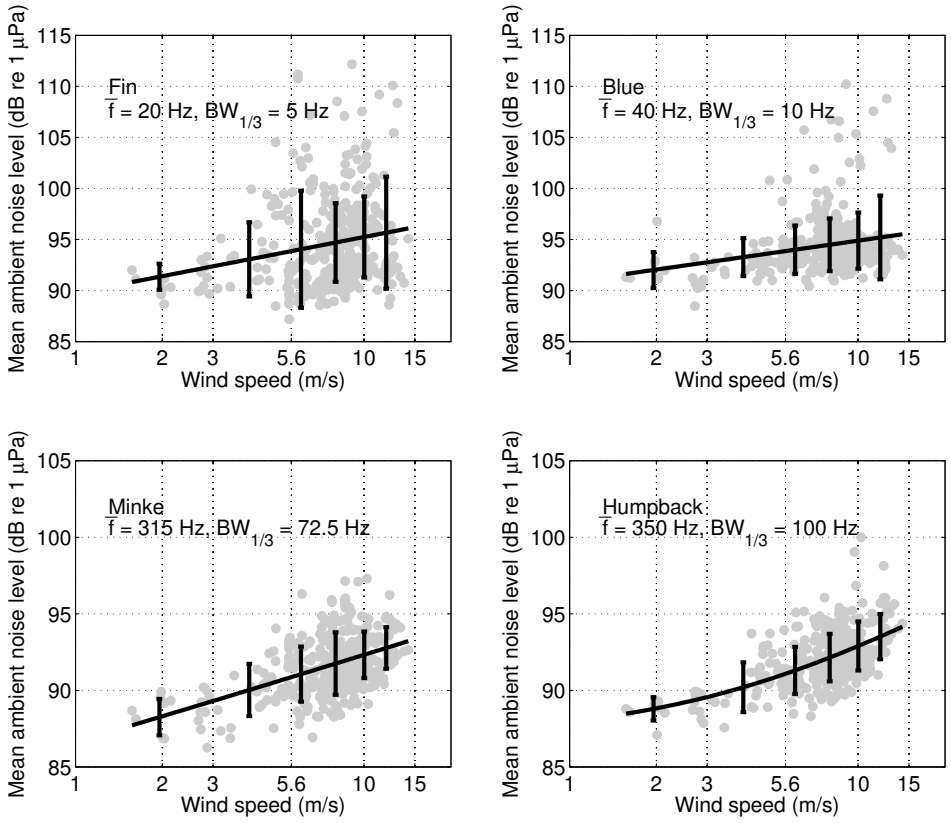

Figure A1. Wind dependence of Gulf of Maine mean ambient noise levels for frequency bands of baleen whale vocalizations given in Table 1. Gray filled circles represent the mean ambient noise levels determined from measurements obtained during the OAWRS 2006 experiment [1,2,22] using Equation (9) for frequency bands of baleen whale vocalizations given in Table 1. Black solid lines represent the empirical best fit of the measured ambient noise levels to the model given in Equation (11). Empirically determined coefficients of the model are given in Table 1. Black vertical lines represent the variation of the measured mean ambient noise levels for given wind speed. Instantaneous measurements of ambient noise fluctuate around each mean ambient noise level with 5.6 dB standard deviation [26].

References

1. Wang, D.; Garcia, H.; Huang, W.; Tran, D.D.; Jain, A.D.; Yi, D.H.; Gong, Z.; Jech, J.M.; Godø, O.R.; Makris, N.C.; et al. Vast assembly of vocal marine mammals from diverse species on fish spawning ground. *Nature* **2016**, *531*, 366–370.
2. Gong, Z.; Jain, A.D.; Tran, D.; Yi, D.H.; Wu, F.; Zorn, A.; Ratilal, P.; Makris, N.C. Ecosystem scale acoustic sensing reveals humpback whale behavior synchronous with herring spawning processes and re-evaluation finds no effect of sonar on humpback song occurrence in the Gulf of Maine in Fall 2006. *PLoS ONE* **2014**, *9*, e104733.
3. Dunlop, R.A.; Noad, M.J.; Cato, D.H.; Stokes, D. The social vocalization repertoire of east Australian migrating humpback whales (*Megaptera novaeangliae*). *J. Acoust. Soc. Am.* **2007**, *122*, 2893–2905.
4. Dunlop, R.A.; Cato, D.H.; Noad, M.J. Non-song acoustic communication in migrating humpback whales (*Megaptera novaeangliae*). *Mar. Mammal Sci.* **2008**, *24*, 613–629.
5. Tyack, P.; Clark, C.W. Communication and acoustic behavior of whales and dolphins. In *Hearing by Whales and Dolphins, Handbook on Auditory Research*; Au, W.W.L., Popper, A.N., Fay, R.R., Eds.; Springer: New York, NY, USA, 2000; pp. 156–224.
6. Edds-Walton, P.L. Acoustic communication signals of mysticete whales. *Bioacoustics* **1997**, *8*, 47–60.
7. Cerchio, S.; Dahlheim, M. Variation in feeding vocalizations of humpback whales *Megaptera novaeangliae* from southeast Alaska. *Bioacoustics* **2001**, *11*, 277–296.
8. Miller, P.J.; Johnson, M.P.; Tyack, P.L. Sperm whale behaviour indicates the use of echolocation click buzzes 'creaks' in prey capture. *Proc. Biol. Sci.* **2004**, *271*, 2239–2247.
9. Johnson, M.; Madsen, P.; Zimmer, W.; De Soto, N.; Tyack, P. Beaked whales echolocate on prey. *Proc. Biol. Sci.* **2004**, *271*, S383–S386.
10. Johnson, M.; Madsen, P.T.; Zimmer, W.; De Soto, N.A.; Tyack, P. Foraging Blainville's beaked whales (*Mesoplodon densirostris*) produce distinct click types matched to different phases of echolocation. *J. Exp. Biol.* **2006**, *209*, 5038–5050.
11. Stimpert, A.; Wiley, D.; Au, W.; Johnson, M.; Arsenault, R. 'Megapclicks': Acoustic click trains and buzzes produced during night-time foraging of humpback whales (*Megaptera novaeangliae*). *Biol. Lett.* **2007**, *3*, 467–470.
12. Overholtz, W.; Link, J. Consumption impacts by marine mammals, fish, and seabirds on the Gulf of Maine–Georges Bank Atlantic herring (*Clupea harengus*) complex during the years 1977–2002. *ICES J. Mar. Sci.* **2007**, *64*, 83–96.
13. Kenney, R.; Scott, G.; Thompson, T.; Winn, H. Estimates of prey consumption and trophic impacts of cetaceans in the USA northeast continental shelf ecosystem. *J. Northwest Atl. Fish. Sci.* **1997**, *22*, 155–171.
14. Weinrich, M.; Martin, M.; Griffiths, R.; Bove, J.; Schilling, M. A shift in distribution of humpback whales, *Megaptera novaeangliae*, in response to prey in the southern Gulf of Maine. *Fish. Bull.* **1997**, *95*, 826–836.
15. Makris, N.C.; Cato, D.H. Using singing whales to track nonsingers. *J. Acoust. Soc. Am.* **1994**, *96*, 3270.
16. Makris, N.C.; Lai, Y.S.; Cato, D.H. Using broadband humpback whale vocalizations to locate nonvocal whales in shallow water. *J. Acoust. Soc. Am.* **1999**, *105*, 993.
17. Lai, Y.S. Acoustic Scattering from Stationary and Moving Targets in Shallow Water Environments—With Application of Humpback Whale Detection and Localization. Ph.D. Thesis, Massachusetts Institute of Technology, The Department of Ocean Engineering, Cambridge, MA, USA, 2004.
18. Frazer, L.; Mercado, E., III. A sonar model for humpback whale song. *IEEE J. Ocean. Eng.* **2000**, *25*, 160–182.
19. Au, W.; Frankel, A.; Helweg, D.; Cato, D. Against the humpback whale sonar hypothesis. *IEEE J. Ocean. Eng.* **2001**, *26*, 295–300.
20. Mercado, E., III; Frazer, L.N. Humpback whale song or humpback whale sonar? A reply to Au et al. *IEEE J. Ocean. Eng.* **2001**, *26*, 406–415.
21. Makris, N.; Ratilal, P.; Symonds, D.; Jagannathan, S.; Lee, S.; Nero, R. Fish population and behavior revealed by instantaneous continental shelf-scale imaging. *Science* **2006**, *311*, 660–663.
22. Makris, N.; Ratilal, P.; Jagannathan, S.; Gong, Z.; Andrews, M.; Bertsatos, I.; Godø, O.; Nero, R.; Jech, J. Critical population density triggers rapid formation of vast oceanic fish shoals. *Science* **2009**, *323*, 1734–1737.

23. Jagannathan, S.; Bertsatos, I.; Symonds, D.; Chen, T.; Nia, H.; Jain, A.; Andrews, M.; Gong, Z.; Nero, R.; Ngor, L.; et al. Ocean Acoustic Waveguide Remote Sensing (OAWRS) of marine ecosystems. *Mar. Ecol. Prog. Ser.* **2009**, *395*, 137–160.
24. Gong, Z.; Andrews, M.; Jagannathan, S.; Patel, R.; Jech, J.; Makris, N.; Ratilal, P. Low-frequency target strength and abundance of shoaling Atlantic herring (*Clupea harengus*) in the Gulf of Maine during the Ocean Acoustic Waveguide Remote Sensing 2006 Experiment. *J. Acoust. Soc. Am.* **2010**, *127*, 104–123.
25. Jain, A.D.; Ignisca, A.; Yi, D.H.; Ratilal, P.; Makris, N.C. Feasibility of Ocean Acoustic Waveguide Remote Sensing (OAWRS) of Atlantic cod with seafloor scattering limitations. *Remote Sens.* **2013**, *6*, 180–208.
26. Makris, N. The effect of saturated transmission scintillation on ocean acoustic intensity measurements. *J. Acoust. Soc. Am.* **1996**, *100*, 769–783.
27. Green, D.; Swets, J. *Signal Detection Theory and Psychophysics*; Peninsula Publishing: Los Altos, CA, USA, 1988.
28. Au, W.; Hastings, M. *Principles of Marine Bioacoustics*; Springer: New York, NY, USA, 2008.
29. Steinberg, B. *Principles of Aperture and Array System Design: Including Random and Adaptive Arrays*; John Wiley & Sons: New York, NY, USA, 1976.
30. Andrews, M.; Gong, Z.; Ratilal, P. High resolution population density imaging of random scatterers with the matched filtered scattered field variance. *J. Acoust. Soc. Am.* **2009**, *126*, 1057–1068.
31. Love, R. Resonant acoustic scattering by swimbladder-bearing fish. *J. Acoust. Soc. Am.* **1978**, *64*, 571–580.
32. Collins, M.D. A split-step Padé solution for the parabolic equation method. *J. Acoust. Soc. Am.* **1993**, *93*, 1736–1742.
33. Chen, T.; Ratilal, P.; Makris, N.C. Mean and variance of the forward field propagated through three-dimensional random internal waves in a continental-shelf waveguide. *J. Acoust. Soc. Am.* **2005**, *118*, 3560–3574.
34. Andrews, M.; Chen, T.; Ratilal, P. Empirical dependence of acoustic transmission scintillation statistics on bandwidth, frequency, and range in New Jersey continental shelf. *J. Acoust. Soc. Am.* **2009**, *125*, 111–124.
35. Wilson, J.D.; Makris, N.C. Ocean acoustic hurricane classification. *J. Acoust. Soc. Am.* **2006**, *119*, 168–181.
36. Tran, D.; Andrews, M.; Ratilal, P. Probability distribution for energy of saturated broadband ocean acoustic transmission: Results from Gulf of Maine 2006 experiment. *J. Acoust. Soc. Am.* **2012**, *132*, 3659–3672.
37. Jagannathan, S.; Küsel, E.T.; Ratilal, P.; Makris, N.C. Scattering from extended targets in range-dependent fluctuating ocean-waveguides with clutter from theory and experiments. *J. Acoust. Soc. Am.* **2012**, *132*, 680–693.
38. Cato, D. Ambient sea noise in Australian waters. In Proceedings of the 5th International Congress on Sound and Vibration, Adelaide, Australia, 15–18 December 1997.
39. Tyack, P. Studying how cetaceans use sound to explore their environment. In *Perspectives in Ethology*; Plenum Press: New York, NY, USA, 1997; Volume 12, pp. 251–297.
40. Kenney, R.D.; Mayo, C.A.; Winn, H.E. Migration and foraging strategies at varying spatial scales in western North Atlantic right whales: A review of hypotheses. *J. Cetacean Res. Manag.* **2001**, *2*, 251–260.
41. Tyack, P.L. Implications for marine mammals of large-scale changes in the marine acoustic environment. *J. Mammal.* **2008**, *89*, 549–558.
42. Jones, F.H.; Scholes, P. Gas secretion and resorption in the swimbladder of the cod (*Gadus morhua*). *J. Comp. Physiol. B* **1985**, *155*, 319–331.
43. MacLennan, D.; Simmonds, E.J. *Fisheries Acoustics*; Chapman and Hall: London, UK, 1992.
44. Nero, R.W.; Thompson, C.H.; Jech, J.M. In situ acoustic estimates of the swimbladder volume of Atlantic herring (*Clupea harengus*). *ICES J. Mar. Sci.* **2004**, *61*, 323–337.
45. Weston, D.E. Sound propagation in the presence of bladder fish. In *Underwater Acoustics*; Albers, V.M., Ed.; Plenum Press: New York, NY, USA, 1967; Volume 2, pp. 55–88.